Journal of Hydrology 460–461 (2012) 143–155

Contents lists available at SciVerse ScienceDirect

Journal of Hydrology

journal homepage: www.elsevier.com/locate/jhydrol

Assessing water availability in a semi-arid watershed of southern India using a semi-distributed model

J. Perrin [a,*], S. Ferrant [b,c,d], S. Massuel [e], B. Dewandel [f], J.C. Maréchal [f], S. Aulong [f], S. Ahmed [g]

[a] BRGM, Water Division, Resource Assessment, Discontinuous Aquifers Unit, Indo-French Centre for Groundwater Research, Uppal Road, 500 606 Hyderabad, India
[b] Université de Toulouse, UPS (OMP), GET, 14 av., Edouard Belin, F-31400 Toulouse, France
[c] IRD, GET, F-31400 Toulouse, France
[d] CNRS, GET, F-31400 Toulouse, France
[e] IRD, UMR G-EAU, BP 64501, F-34394 Montpellier Cedex 5, France
[f] BRGM, Water Division, NRE Unit, 1039 rue de Pinville, 34000 Montpellier, France
[g] National Geophysical Research Institute, Indo-French Centre for Groundwater Research, Uppal Road, 500 606 Hyderabad, India

ARTICLE INFO

Article history:
Received 16 November 2011
Received in revised form 19 June 2012
Accepted 1 July 2012
Available online 7 July 2012
This manuscript was handled by Philippe Baveye, Editor-in-Chief, with the assistance of Xunhong Chen, Associate Editor

Keywords:
Water resource management
SWAT
Semi-arid
Crystalline aquifer
India
Irrigation

SUMMARY

Appropriate groundwater resource management becomes a priority for the States of the semi-arid southern India. Because of the highly increasing groundwater demand, the number of drought-prone regions where the groundwater resource is classified as over-exploited by the Government is critically increasing. Thus there is a need to develop quantitative methodologies adapted to the regional context that are capable to assess water resources at watershed scale and the impact of management measures. This study demonstrates the calibration and use of an integrated water resource assessment model (SWAT) in an 84 km^2 representative semi-arid crystalline watershed of southern India with no perennial surface water source. The model can reproduce (i) the recharge rate estimates derived independently by a groundwater balance computation, (ii) runoff and surface water storage occurring in tanks that spread along the drainage system, (iii) groundwater table fluctuations monitored at a monthly time step. Results show that even if the calibration period (2006–2010) was more humid than long-term average, the watershed is sensitive to the monsoon inter-annual variability with water-stress during the dry years and an associated loss in agricultural production. The impact of these dry years is spatially variable with higher vulnerability for sub-basins having proportionally larger irrigated paddy areas, lower groundwater resource, and/or lower recharge potential (i.e., due to land use and repartition of percolation tanks). The scope for additional recharge by means of managed aquifer recharge structures is limited and demand-side management measures are needed to mitigate pumping. A wishful management objective may be to see groundwater reserves as a supplementary resource in case of monsoon failure and not as the main water resource to be used indiscriminately.

SWAT proved to be an adequate modeling framework for the simulation of water resource in semi-arid hard-rock context where groundwater vertical fluxes largely prevail over regional lateral flows at km-scale. It provides interesting capabilities for water availability mapping and the simulation of different types of scenarios (e.g., land use changes, climate change).

1. Introduction

Large swaths of the south Indian peninsula are particularly prone to droughts because of the specific geo-climatic setting (semi-arid hard-rock region with a potential annual evapotranspiration of 1800 mm, an aridity index of 0.42, and a high inter-annual variability in monsoon rainfall) and the intensive use of the groundwater resource for agriculture (e.g., World Bank, 2010). This situation makes rural communities particularly exposed to climatic variability and argues for the implementation of sound water resource management policies. So far, both State and Federal governments have favoured supply-side management measures such as building-up of reservoirs, transfer of surface water, rainwater harvesting structures (percolation tanks, check dams), managed aquifer recharge (e.g., Central Ground Water Board, 2005, 2007; Sakthivadivel, 2007). Despite the potential positive impact of these measures on rural community livelihoods (e.g., Glendenning and Vervoort, 2011), there is a serious need for quantitative assessment of the impact of these management measures at catchment scale (Kumar et al., 2006; Sakthivadivel, 2007). Water resource management tools and models adapted to the local context may prove very

* Corresponding author. Tel.: +91 99 49 09 56 44; fax: +91 40 23 43 46 51.
E-mail addresses: je.perrin@brgm.fr (J. Perrin), sylvain.ferrant@lmtg.obs-mip.fr (S. Ferrant), sylvain.massuel@ird.fr (S. Massuel), b.dewandel@brgm.fr (B. Dewandel), shakeelahmed@ngri.res.in (S. Ahmed).

0022-1694/$ - see front matter © 2012 Elsevier B.V. All rights reserved.
http://dx.doi.org/10.1016/j.jhydrol.2012.07.002

useful for the evaluation of different management strategies (land-use, recharge), climatic scenarios, and vulnerability mapping. Such outputs should help guiding policy-makers in their choices towards a sustainable management of the water resource. The implications of such developments go beyond water resource management and encompass rural community vulnerability assessment (e.g., O'Brien et al., 2004), food production (e.g., Faramarzi et al., 2010) and food security (Kumar, 2003), socio-economic development (Kay et al., 1997), and also energy demand management (Kumar, 2005; Mukherji, 2007; Shah et al., 2008).

Research activities aiming at the development and application of groundwater resource management tools have gained momentum over the recent years in line with needs expressed by planners and policy-makers: estimation of the impact of groundwater pumping on water balance in a semi-arid context (Ruud et al., 2004), groundwater recharge spatial variability in a humid hard-rock context (Dripps and Bradbury, 2010), the estimation of net groundwater use in a semi-arid alluvial context (Ahmad et al., 2005).

In India, research on water resource estimation at catchment scale have focused on the estimation of actual evaporation using satellite imagery (Bouwer et al., 2008), the calibration of an hydrological model using actual evaporation derived from satellite imagery (Immerzel and Droogers, 2008), a modeling approach focusing on surface water irrigation and their associated return flow (Gosain et al., 2005); however these studies are mostly limited to surface water.

Groundwater studies have been devoted to field-based recharge estimation as the most crucial groundwater balance component in the semi-arid context (e.g., Rangarajan and Athavale, 2000; Sukhija et al., 2003), the development of a methodology for quantitative groundwater balance computation adapted to semi-arid hard-rock aquifers (Maréchal et al., 2006), a groundwater recharge model for the southern Indian rural context which enables to test the evolution of groundwater resource according to land use change (Anuraga et al., 2006), groundwater modeling in a large irrigation system (Chowdary et al., 2003). A Decision Support Tool was designed for the groundwater resource management in hard-rocks (Dewandel et al., 2007, 2010).

Recently, Glendenning and Vervoort (2011) developed a water balance conceptual model designed to estimate the impacts of rainwater harvesting on the catchment hydrology in Rajasthan and applicable to scarce field data contexts.

These existing studies focus on either surface water or groundwater and studies presenting an integrated modeling framework are lacking. With such an approach the temporal evolution of water availability, that is groundwater storage and surface storage in tanks and soil, will be evaluated.

The objective of this study is to calibrate an integrated model capable of evaluating both surface and groundwater resources in a representative semi-arid crystalline watershed of southern India experiencing groundwater over-exploitation, compare the spatial variability and the temporal evolution of the different water fluxes and storage within the watershed, and evaluate the potential for water resource management options. To do so, extensive field work was carried out in the selected watershed for an accurate characterization of the surface and groundwater storage components (percolation tanks and aquifer geometry) and the quantification of water fluxes (recharge, pumping, rainfall, etc.).

2. Study area and data

2.1. Climatic and geological context

The present study focuses on a representative hard-rock semi-arid watershed where groundwater is intensively pumped for irrigated agriculture (Gajwel watershed, 84 km^2, Andhra Pradesh, Fig. 1a). The area is characterized by a relatively flat topography 520–620 m above sea level and the absence of perennial streams. Surface streams are dry most of the time, except after heavy rainfall events during the monsoon. The region experiences a semi-arid climate controlled by the periodicity of the monsoon: rainy or "Kharif" season from June to October and dry or 'Rabi' season from November to May. Mean annual rainfall is 812 mm, 88% falling during the monsoon (AP Handbook of Statistics data). The mean annual temperature is 26 °C, although the maximum temperature in summer can reach 45 °C.

The area includes 10 villages with a total population of about 36,130 inhabitants (Indian Census 2001). The main economic activity is agriculture with cultivation of irrigated crops (mainly paddy rice, some vegetables), rainfed crops (maize, cotton) and breeding of livestock and poultry. The primary source of irrigation is groundwater and intensification of irrigation since 1990 has led to the over-exploitation of the groundwater resource (over 1200 borewells in use, AP Groundwater Department, pers. com.) and decreasing trends in piezometric levels. This present situation limits natural regional groundwater flow (e.g., Dewandel et al., 2010). A cascading tank system is maintained along the main surface drainage channels. Traditionally, these village tanks were the main water source for communities during the long dry season, but presently their main role is to retain runoff in the watershed and contribute to additional recharge to the aquifer (percolation tanks).

The Gajwel area is underlain by orthogneissic Archean granite commonly found in the region with some intrusive rocks locally (leucocratic granite, dolerite dykes, quartz reefs).

The weathering profile is a few tens of meters thick and very similar to the one known in the Hyderabad surroundings (e.g., Dewandel et al., 2006). The aquifer is within the weathering profile and constituted by two layers having contrasted hydrodynamic properties (Dewandel et al., 2006): the saprolite layer with a low hydraulic conductivity and a higher porosity (1–5%) and the underlying fissured layer with a higher hydraulic conductivity and a lower porosity (0.5–1%).

2.2. Field data

Field data needed for the modeling include daily meteorological data, land cover/land use map, soil map, digital elevation model of the watershed, soil physical properties, groundwater reservoir geometry (Fig. 2a), surface reservoir geometry, water extraction. The sub-basin delineation is defined by the user (Fig. 2a) using the 90-m grid size SRTM digital elevation model (DEM).

Rainfall data are measured at daily time step within the town of Gajwel (Mandal Revenue Office) from 2000 to 2010. Other meteorological parameters (temperature, windspeed, solar radiation, humidity) are from the nearest complete meteorological station located at Patancheru (ICRISAT campus) 60 km SW of Gajwel.

The watershed surface outlet is not monitored but is known to flow only after intense rainfall; thus it is dry most of the time. Runoff is captured by tanks (32 tanks in total, Fig. 1a), which correspond to surface water flow accumulation behind locally made earth dam structures along main drainage routes. These tanks can be used as an efficient way to estimate the amount of runoff occurring in the watershed. Six tanks were surveyed to determine the relationship tank area-storage volume using two different methods. With the first method, tank limits were mapped based on the GPS-tracking of the water surface at regular time intervals during depletion so as to obtain elevation contours (tanks 6, 10, 31). With the second method, the tank bottom was leveled using a Differential-GPS (Trimble®) when tank was empty (tanks 4, 5, 27). In both cases, elevation data points were interpolated using the TIN method and then tank volume and surface area were

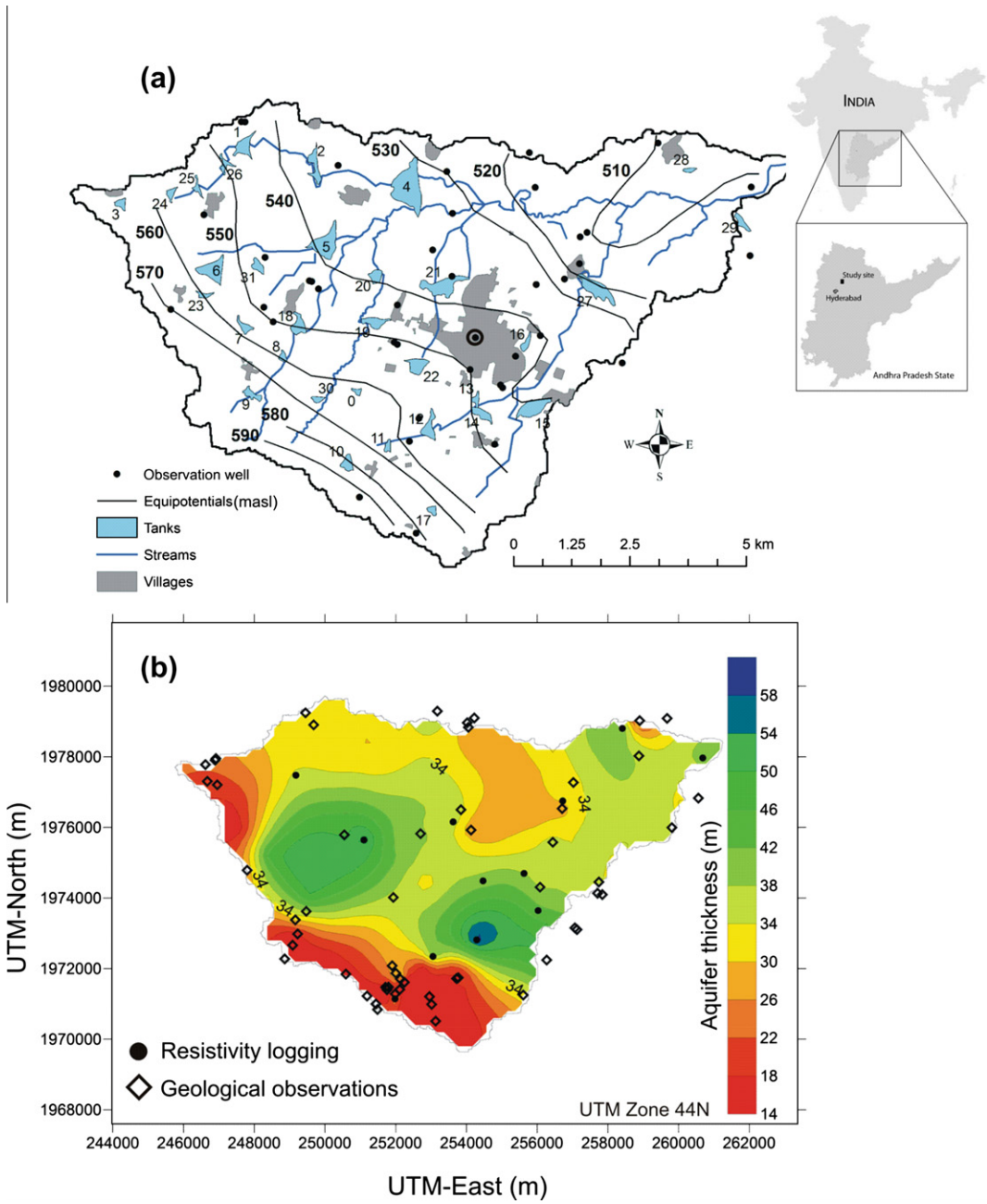

Fig. 1. (a) Location of the study area and map of Gajwel experimental watershed showing the water-table contours (June 2010 campaign), tanks with their ID, main seasonal streams; the Government monitoring piezometer location is marked by a circle. (b) Aquifer thickness map with geological and geophysical observation points.

calculated for any altitude of the water surface on a 10 cm-increment basis (ArcGIS®).

The watershed soil map (Fig. 2b) was modified from the published map (1:500,000, NBSS, 2000) using satellite imagery and field verifications. Two soil types belonging to the Alfisol order are dominant: a montmorillonitic Ustrop named black soil and a clayey-skeletal typical Ustropepts named red soil in this study. The soil spatial distribution clearly indicates a close relationship between topography and soils: the black soils are located in the valley floors and in the downstream part of the watershed.

The watershed land-use map (Fig. 2c) was compiled using multispectral satellite images (two images in March 2007 and 2010 for the Rabi season and two images in December 2007 and October 2009 for the Kharif season) from LISS IV sensor onboard the Resourcesat-I (IRS 1D) satellite. The multispectral satellite image from the LISS IV sensor contains three spectral bands, i.e., Green (0.5–0.6 μm), Red (0.6–0.7 μm), and Near Infrared (0.7–0.9 μm). The pixel size for all bands is 5.8 m. The used digital elevation model (DEM) is the free SRTM 90-m resolution.

The land cover includes 27% (2261 ha) of rainfed crops (corn and cotton) situated generally within the black soil areas (Fig. 2b and c), 6.3% (533 ha) of irrigated rice paddies cultivated twice a year, 2.5% (213 ha) of irrigated paddies cultivated only during Kharif (remains as bare soil the rest of the year), 1.1% (90 ha) of irrigated orchards, 5.1% (432 ha) of built-up areas, 6.7% (561 ha) of forest (mainly eucalyptus plantations) and 48.2% (4054 ha) of semi-arid scrubland used for extensive grazing. The total tank surface area covers 3.1% (259 ha) of the watershed.

Representative daily irrigation, estimated from field surveys (measurements of instant well discharge, irrigated field area, and

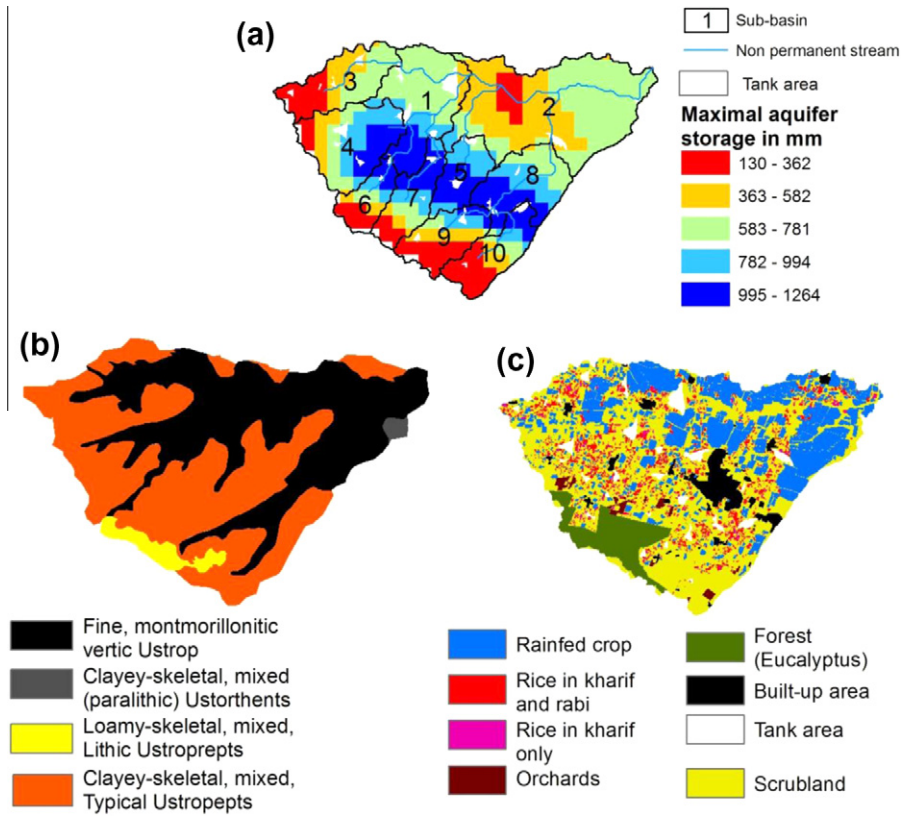

Fig. 2. (a) Repartition of the 10 sub-basins used for SWAT modeling and discretization of the aquifer maximum storage capacity; (b) soil map and (c) land use map used for SWAT modeling.

monitoring of daily pumping duration (Massuel et al., 2008)), is 12 mm/day and 9 mm/day for Rabi and Kharif rice respectively (Perrin et al., 2008). The crop calendar for each land cover may vary up to one or 2 weeks for rainfed crops from 1 year to the next. Water extraction for domestic use is estimated on the basis of population figures (Indian Census 2001).

In some places, farmers also cultivate irrigated vegetables either during Rabi season or between two crops of paddy to maximize the groundwater use. However these practices could not be incorporated in the model as it is not possible to differentiate between irrigated crops from the satellite imagery. The irrigated area extent is also known to vary between dry years and humid years, in relation to the available pumped groundwater and the farmers' perception of the coming monsoon. However this land use temporal variability could not be tracked on the limited number of available satellite images. We have used the governmental statistics of season-wise irrigated areas (Handbook of statistics from 2000 to 2008) and a farmers' socioeconomic survey carried out in the watershed to infer the relative variation of the irrigated areas for the simulation period. In practice, a static land use (Fig. 2c) corresponding to the maximal cultivated areas is implemented in the model, and the daily amount of irrigation is adjusted to fit historical irrigated areas (i.e., less irrigation during seasons for which a reduction in irrigated areas was recorded).

The groundwater reservoir capacity was computed using the aquifer thickness map (Fig. 1b) and aquifer porosity values of 1% for the entire fissured layer and 3% for the saprolite layer (Dewandel et al., 2006, 2012). The map is made on the basis of geological observations at outcrops and defunct dug wells (130) completed by a geophysical survey (resistivity logging in twenty borewells). This groundwater reservoir capacity (or maximal groundwater storage) defines the threshold below which no base flow from groundwater contributes to stream flow.

3. Methodology

3.1. Groundwater balance

A groundwater balance at watershed scale is computed independently of the model to provide estimates of groundwater recharge to be used for model calibration. A robust approach for the regional context is the double water table fluctuation technique (Maréchal et al., 2006). The groundwater balance can be expressed as follows:

$$R + RF + Q_{in} = E + P + Q_{out} + \Delta S \quad (1)$$

With:

$$\Delta S = S_y \cdot \Delta h \quad (2)$$

where R is the recharge (mm/season), RF is the irrigation return flows (mm/season), Q_{in} and Q_{out} are the groundwater fluxes across the watershed boundaries (mm/season), E is the revaporation from the water table (mm/season), P is the groundwater pumping (mm/season), ΔS is the seasonal change in groundwater storage (mm/season), S_y is the specific yield (or effective porosity), Δh is the water table fluctuation. In over-exploited crystalline aquifers, Q_{in} and Q_{out} are very small fluxes known to balance each other (Maréchal et al., 2006; Dewandel et al., 2010), therefore the two terms can be neglected in Eq. (1).

Eq. (1) is solved twice a year: once for the dry season where R is 0 and the equation is solved for S_y (the other terms being determined using field data), once for the monsoon season where R is computed using S_y computed in the dry season.

RF is computed using a daily water balance at field scale for estimating water available for deep infiltration coupled with a variably saturated 1D vertical flow model that computes the downward vertical water flux below the soil depth (Dewandel

et al., 2008). The computation is made for soil hydrodynamic properties and irrigation practices that are representative at watershed scale. The model is run on a daily time step with daily irrigation and meteorological parameters as inputs and daily return flows are then averaged over the entire season to obtain the term *RF*. *E* is computed using the empirical relationship of Coudrain-Ribstein et al. (1998) which relates the revaporation with the thickness of the unsaturated zone. *P* is estimated using land use mapping to determine the entire irrigated surface area coupled with field measurements of irrigation practice to determine the irrigation rate; the data are consistent with the number of borewells in use in the watershed (Perrin et al., 2008). The seasonal water table fluctuation (Δh) is determined from two piezometric campaigns per year, one at the end of the dry season, one at the end of the monsoon, including 40–60 piezometers (usually abandoned farmer wells, Fig. 1a). Measured data are interpolated using the kriging method to obtain a representative average seasonal water table elevation at watershed scale. Preliminary tests made on the effect of the grid size (200, 400, 800-m) on the computed average water table showed a minimal impact (less than 1% difference). Final computations were carried out using a 200-m grid size. The density of observation wells will also influence the results with higher degree of representativeness reached using more observation points. However, by a geostatistical study in a similar watershed, Zaidi et al. (2007) showed that the optimal number of observation wells is around 50 (i.e., no significant improvement in accuracy is observed with a higher number).

3.2. Modeling tool and simulated water transfers

The SWAT (Soil and Water Assessment Tool) was selected as the integrated modeling tool because of its robust approach of soil water balance at the watershed scale. It has been applied to a broad range of conditions for which limited observations may be available and is widely used to study the impacts of environmental changes (e.g., Bouraoui et al., 2004; Chaplot, 2007; Eckhardt and Ulbrich, 2003; Rosenberg et al., 2003). This model (Arnold and Allen, 1996; Borah and Bera, 2004) is a process-based, basin-scale, continuous-time model that operates at a daily time step and was designed to assess the long term impact of land management on water balance, sediment transport and nonpoint source pollution in large river basins. The spatial unit is the sub-catchment that is further divided into hydrologic response units (HRUs) (Neitsch et al., 2002), a sub-unit defined by overlaying soils, land use and slope maps. Most soil and aquifer computing is done at the HRU scale and results are integrated at the sub-basin scale. The soil and crop model is mainly based on the Erosion and Productivity Impact Calculator (EPIC) from Williams et al. (1984), a field scale model where sowing, irrigation frequency and amount, tillage and harvesting information can be detailed.

The vertical water budget includes:

1. Evapotranspiration from soil moisture and surface water depending on land cover, crop succession and irrigation application. This flux is evaluated on the basis of the generic crop module. The plant evapotranspiration rate in function of the plant development is computed on the basis of a potential evapotranspiration estimated using Penman–Monteith equations.
2. Percolation (i.e., the amount of water seeping out of the lowest soil layer) which is controlled by infiltration, soil layers permeability and evapotranspiration uptake.
3. Recharge (*R*) which is the sum of percolation and other contributions from the sub-basin: runoff transmission losses and reservoir seepage (see below).
4. Revaporation (*E*) out of the shallow aquifer into the soil zone in response to water deficit; this flux is activated when the water table is higher than a threshold defined by the user.

The horizontal water transfers include:

1. Daily surface runoff evaluated using the empirical curve number approach (USDA-SCS, 1972).
2. Base flow from the shallow aquifer to the river, occurring only when groundwater table is connected to the river.
3. Lateral flow or sub-surface flow which originates below the surface but above the saturated zone contributing to streamflow, and is controlled by the vertical variation in hydraulic conductivity, slope and soil water content in each soil layer. The study site is flat, and no impermeable layer have been described in the several Alfisoil found in the catchment. Thus, lateral flow is supposed to be negligible.

These horizontal water transfers are computed at the HRU scale. The hydrological model is semi-distributed, meaning that each horizontal water transfer goes directly to the stream, irrespective of the HRU position in the sub-basin.

The watershed is divided into 10 sub-basins (Fig. 2a), each of them having one surface reservoir (except the downstream one) collecting runoff generated within the sub-basin.

In SWAT, the groundwater reservoir is supposed to be perfectly connected within a sub-basin and independent from each adjacent sub-basin (i.e., no lateral groundwater flow exchange possible between sub-basins). In Gajwel watershed, lateral groundwater flow exists between sub-basins as shown by the water table contour map (Fig. 1) and also across the watershed boundaries. A quantitative estimation of these lateral groundwater flows remains hypothetical because detailed field information would be required: individual pumping rates, hydraulic conductivity spatial distribution which is locally highly variable in such heterogeneous media, lateral variations in cross-sectional flow areas, local hydraulic gradients. However, an assessment of lateral groundwater flow across hydraulically connected sub-basins was performed using Darcy flow velocity and cross-sectional flow areas (i.e., the saturated aquifer thickness multiplied by the respective width of the lateral connections). It showed that maximum lateral flow rates across sub-basins boundaries are in the same range as the flow rate of a single pumping well. Since on average each sub-basin has about 120 pumping wells, lateral flows are small ($\sim$1% of pumping rates). Moreover they are likely to balance at least partly each other since most sub-basins will be fed by up-gradient lateral flow and feed down-gradient sub-basin (i.e., because of the regional water table that follows the topography). Similar observations were made in the local context where crystalline aquifer of low horizontal hydraulic conductivity (10^{-5} m/s) with a high density of pumping leads to the preponderance of vertical water fluxes (pumping, evaporation, recharge) over lateral fluxes (Maréchal et al., 2006; Dewandel et al., 2010). This dominance of vertical fluxes was verified by Dewandel et al. (2012) using a coarse-graining method. For a similar watershed in southern India, they showed that for cells size above 520×520 m, lateral flows balance each other and therefore the lateral flow component can be neglected for groundwater balance computation. In other words, if lateral flow exists as suggested by piezometric heads (Fig. 1a), it is either small compared to vertical flow or in-flow counterbalances out-flow (which is similar to no flow for groundwater budgeting). It means that the use of the SWAT model is adapted to local field conditions provided that modeled sub-basins are not too small.

Streams and surface water harvesting systems are simulated by SWAT. Sub-basin streams are composed by tributary channels draining into a main channel. The geometry of such flow paths

are computed with GIS tools based on the DEM. As the streams are intermittent in such semi-arid areas, groundwater is disconnected from the streambed and losses of surface flow as percolation across the streambed are possible (i.e., transmission loss). SWAT uses Lane's method to estimate this percolation (USDA-SCS, 1983). The water harvesting system is composed by tanks (i.e., small reservoirs) spreading along the intermittent streams that will collect surface flow up to a maximal capacity defined by the geometry of each tank. SWAT simulates one reservoir for each sub-basin. Therefore the actual percolation tanks located in each sub-basin are aggregated into a single synthetic reservoir by adding up surface and storage volume of each individual tank.

The Rice paddy system is simulated as a daily irrigated crop in a way that minimizes runoff. The seepage in the first soil layer fills the available water capacity and is extracted by the evapotranspiration of the growing rice. Excess water percolates out of the soil as return flow to the shallow aquifer.

3.3. Calibration and validation methodology

Because no discharge time series are available and river are not permanent, the calibration was performed on the several aquifer recharge processes evaluated independently by field studies at seasonal scale from 2006 to 2010.

The validation process is carried out on monthly piezometric variations recorded by the State Groundwater Department in Gajwel town for the period 2000–2010. Additional validation for runoff processes is obtained by comparing the evolution of simulated and observed tank storages for the period 2007–2009 (i.e., corresponding to the tank monitoring period).

4. Results

4.1. Surface reservoir geometry and dynamics

The relationship tank area-tank storage volume for the six surveyed tanks can be reproduced by a polynomial curve with a RMSE of 5.0% (Fig. 3). The limited variability of tank geometry may be explained by the rather homogeneous topography in the watershed and the systematic locations of tanks along the main drainage axes.

The maximum area of the 32 tanks scattered within the watershed (Fig. 1a) is determined from satellite imagery interpretation and topographical maps (1/50,000 scale, Survey of India). For each tank the maximum storage capacity is computed using the model except for the six surveyed tanks for which field data are used. Since only one reservoir per sub-basin can be represented in the SWAT model, individual tank area and storage volume are aggregated to determine SWAT reservoirs characteristics (Table 1). Tanks 28 and 29 located in the downstream sub-basin are discarded as they are disconnected from the drainage system, their storage capacity is low, and moreover tank 29 is on the edge of the watershed (Fig. 1a). Uncertainty on the reservoir maximum storage volume is not easily assessed as it will depends on the number and size of individual tanks (e.g., larger tanks are better simulated by the exponential model), the number of surveyed tanks in the aggregated reservoir, local topography, etc. These factors have been taken into account to estimate the individual relative error on the reservoir maximum volume (Table 1); at the watershed scale, the total storage capacity is 533×10^4 m^3 ± 8%.

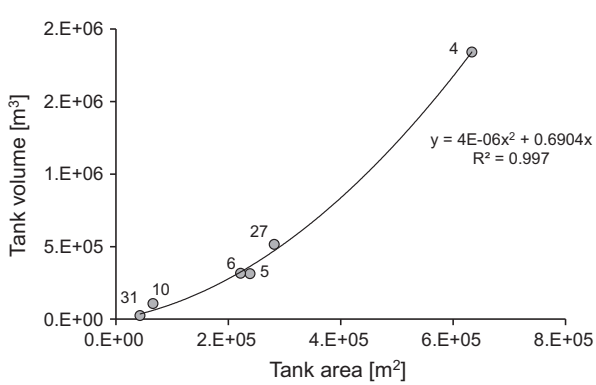

Fig. 3. Tank area – volume relationship for the six tanks surveyed along with the fitted model. Each point represents the maximum area and volume determined from field survey and the numbers corresponds to the tanks ID (location in Fig. 1a).

Table 1
Maximum surface area and storage capacity of each reservoir; except for reservoir 6, each of them is a composite of several percolation tanks located in Fig. 1. The total storage capacity at watershed scale is 533×10^4 m^3 ± 8%.

SWAT reservoir ID	Reservoir max. area (ha)	Reservoir max. storage volume (10^4 m^3)	Percolation tanks[a]
1	41.5	42.2 ± 15%	1, 2, 3, 24, 25, 26
2	59.5	72.5 ± 5%	**5**, **6**, 7, 23, **31**
3	39.6	63.2 ± 15%	21, 22
4	20.6	20.5 ± 15%	8, 9, 18
5	23.3	22.1 ± 15%	0, 19, 20, 30
6	63.3	184.1 ± 1%	**4**
7	33.7	37.7 ± 15%	**10**, 11, 12, 13, 14
8	24.6	35.7 ± 15%	15, 17
9	33.0	55.3 ± 5%	16, **27**

[a] Refers to tank ID Fig. 1, in bold the tanks that have been surveyed.

The water level of one tank (tank 10) was monitored during two hydrological years. In addition, the depletion rate of three more tanks (tanks 6, 19, 31) was monitored during the fall 2008–2009. Observed depletion rates are 15.6, 17.6, 17.0, 20.4 mm/day for tanks 6, 10, 19, 31 respectively. Depletion is mainly caused by evaporation and percolation fluxes (Perrin et al., 2009; Massuel et al., in preparation). Since evaporation fluxes are expected to be within the same range at watershed scale, most of the observed depletion variability is attributed to percolation (silting, hydraulic gradients in the tank surroundings). The mean evaporative fluxes for the period October 2008–January 2009 are 5.3 mm/day based on evaporation pan measurements. If a depletion rate of 16–17 mm/day is assumed to be more representative of tanks of significant size (i.e., such as tanks 6 and 10) and other uptakes such as livestock are less than 1 mm/day, percolation fluxes are 10.2–11.2 mm/day, thus accounting for 62–68% of the observed depletion.

4.2. Groundwater balance at watershed scale

Results of the groundwater balance with associated uncertainties for the period 2006–2010 are given in Table 2. S_y could be quantified for 2 years only (2006–2007 and 2009–2010) as the dry season 2008 experienced an unusual recharge event in March (during the dry season) and for the dry season 2009, the maximum water table elevation remained unknown because the piezometric campaign was carried out too early in October. The average S_y (0.014), consistent with previous studies in similar context (e.g., Maréchal et al., 2006), was used to compute R.

Uncertainties on the different budget components were computed as follows: uncertainties on RF, namely on the return flow coefficient, are issued from the variability of paddy soil hydraulic conductivity, Dewandel et al. (2006) evaluated the relative uncertainty at ±7.4% for the Rabi season and ±14.6% for the Kharif season; uncertainties on E are directly computed from the

Table 2
Annual groundwater balance at watershed scale based on the double water table fluctuation method (Maréchal et al., 2006).

	Total rainfall (mm)	Monsoon rainfall (mm)	R (mm)	RF (mm)	PG (mm)	E (mm)	ΔS (mm)	S_y
June 2006–May 2007	881	765	104 ± 23	61 ± 8	127.6 ± 12.8	0.82 ± 0.20	36.9	0.014
June 2007–May 2008	754	551	40 ± 21	81 ± 8	141.8 ± 12.8	0.74 ± 0.18	−21.9	[a]
June 2008–May 2009	806	788	80 ± 24	108 ± 8	206.5 ± 12.8	0.74 ± 0.20	[a]	[b]
June 2009–May 2010	682	523	85 ± 23	103 ± 6	206.5 ± 12.8	0.67 ± 0.17	−19.9	0.014
June 2010–November 2010[b]	927	897	165 ± 34	67 ± 7	98.1 ± 6.8	0.48 ± 0.25	[c]	[c]

[a] Budgeting not possible due to exceptional recharge occurring in March 2008.
[b] Piezometric campaign carried out too early in October 2008.
[c] Only monsoon season.

uncertainty on the water table elevation (see below); uncertainties on P are taken as ±5.5% based on the study of Maréchal et al. (2006) who compared for another similar watershed the method used in the present study (i.e., combination of land use and field survey) with a complete set of discharge measurements in the field. Uncertainties on the mean water table elevation from kriging are computed from the standard deviation of residuals and are comprised between 0.5 and 1.2 m. The uncertainty on R is the sum of all uncertainties on the parameters used in the computation.

4.3. SWAT modeling

4.3.1. Calibration

Four sub-systems need to be parameterized in the SWAT model: soil, groundwater, surface reservoirs and runoff (Table 3). The so-called "fixed" parameters were determined from field observations and the so-called "calibrated" parameters were tuned during the calibration procedure.

The range of each calibrated soil parameters was defined using a previous study (De Condappa, 2005) for texture, available water capacity (SOL_AWC) and hydraulic conductivity (SOL_K). The groundwater parameters REVAPMN and GW_REVAP were tuned to limit the transpiration from the groundwater table through the capillarity fringe so as to match field-derived revaporation data (E) (Table 2). The parameter GW_DELAY, which controls the ratio between delayed and rapid recharge, was fitted on monthly piezometric data. The reservoir bottom hydraulic conductivity (RESK) was tuned to reproduce the observed ratio between reservoir evaporation and deep percolation (see Section 4.1). For surface runoff, the curve number (CN) was fitted so as to reproduce observed reservoir fillings.

Simulated annual aquifer recharge is constituted of return flow (Fig. 4a) and recharge under non-irrigated areas (Fig. 4b) which is the sum of natural recharge and tank seepage. The modeling results were compared with the estimated recharge from the groundwater balance at watershed scale and the return flow computed using the field water balance and variably-saturated flow model of Dewandel et al. (2008) (Table 2). The simulated recharge under non-irrigated areas (Fig. 4b) is in the range of the estimated recharge. The simulated recharge in 2008 is 50 mm more than the higher bound of the estimated recharge. This difference is largely explained by the fact that the estimated recharge based on observed piezometric fluctuations does not take into account the unusual recharge of March 2008 that has produced around 40 mm of additional recharge. The model underestimates the recharge that occurred in 2009 estimated from piezometric data.

The simulated return flow is in the range of the estimations presented in Table 2. The model underestimates the return flow in Rabi season 2008 (32 mm against 60 mm estimated) and during the Rabi 2009 and 2010 (respectively 33 mm instead of 48 mm and 24 mm instead of 55 mm).

Each simulated recharge (natural recharge, tank seepage, and return flow) were aggregated into a total annual aquifer recharge (Fig. 4c). The simulated total recharge is slightly higher than total recharge estimated from field observations with the exception of the dry year 2009 where the model underestimates recharge. The larger difference observed for the year 2008 is partly due to exceptional recharge occurring during the dry season that could not be computed by the double water table fluctuation technique (lack of data).

The runoff and reservoir parameters calibration is illustrated by the fitting of observed storage in tank 10 and simulated reservoir storage in corresponding sub-basin 9 (Fig. 5). Since tank 10 surface

Table 3
Fixed and calibrated parameters with their respective ranges for the different sub-systems (soil, groundwater, surface reservoirs, runoff) of the model.

		Description	Final values
Soil parameters			
Fixed	SOL_Z	Soil thickness (mm)	1000–2500
Calibrated	SOL_AWC	Available water capacity of the soil layer (mmH_2O/mm soil)	0.3 top to 0.1 bottom
	SOL_K	Saturated hydraulic conductivity (mm/h)	1–3
Groundwater parameters			
Fixed	SHALLST	Groundwater initial storage (mmH_2O)	From piezometry 2006
	GWQMN	Maximum groundwater storage (mmH_2O)	See Table 2
Calibrated	REVAPMN	Threshold depth of water in the shallow aquifer for "revap" (mmH_2O)	350–500
	GW_REVAP	Groundwater "revap" coefficient	0.02
	GW_DELAY	Groundwater delay coefficient (days)	2
Reservoir parameters			
Fixed	RES_ESA	Maximum reservoir surface area (ha)	See Table 1
	RES_EVOL	Maximum reservoir storage volume (10^4 m^3)	See Table 1
Calibrated	RESK	Hydraulic conductivity of the reservoir bottom (mm/h)	0.3
Surface runoff parameters			
Calibrated	CN	Curve number	35–75

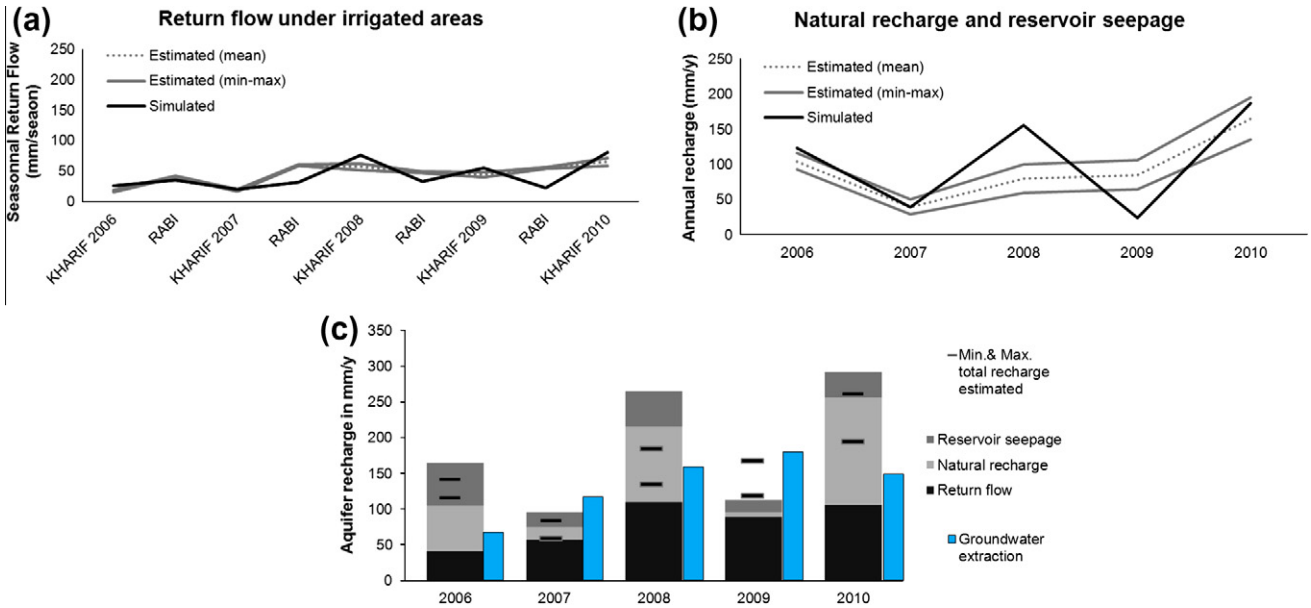

Fig. 4. Comparison of (a) irrigation return flow simulated (black line) and estimated (gray lines) using the groundwater balance, (b) natural recharge and tank seepage simulated (black line) and estimated (gray lines) using the groundwater balance, (c) the different simulated recharges and the corresponding groundwater extraction at watershed scale.

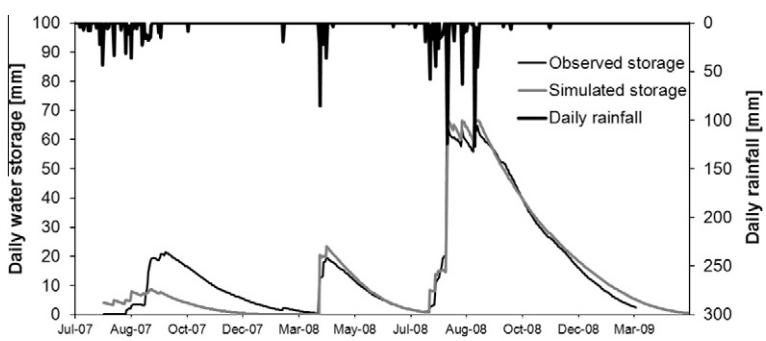

Fig. 5. Observed vs. simulated tank water storage (tank 10, sub-basin 9) and daily rainfall measured in the watershed.

corresponds to 24% of the total tanks surface in sub-basin, a ratio of 0.24 was applied to the sub-basin reservoir volumes. The storage dynamics depends on the reservoir filling by runoff on the one hand, and evaporation and seepage fluxes depleting the reservoir on the other hand. The calibrated model reproduces well the reservoir storage dynamics for the March 2008 storm and the monsoon 2008; in contrast the monsoon 2007 is poorly simulated with only 25% of the observed runoff being simulated.

4.3.2. Validation

The temporal evolution of simulated groundwater storage at watershed scale was compared with measured monthly piezometric levels in Gajwel town (AP Groundwater Department) for the validation period 2000–2010 (Fig. 6). To do so, piezometric data were converted in groundwater storage in mm using the known aquifer thickness (Fig. 1b) and specific yield at the piezometer location. A reasonably good fit is obtained (RMSE = 19.7%) with the right timing for recharge and the right amplitude for wet years. Observed depletions on the piezometer during the Rabi seasons may be accentuated by local pumping and therefore not reflected in the simulated storage. The model does not generate enough recharge for drier monsoons with significantly lower simulated storage gains as already shown when comparing recharge fluxes.

Differences between modeled values and observations (runoff) or recharge estimates from the groundwater balance (natural recharge, return flow) could not be reduced further by additional calibration procedure.

4.3.3. Modeling results

On average for the simulated period (2000–2010), annual rainfall is 775 mm (37 mm less than the long-term average) and it is consumed by the following components (Fig. 7): evapotranspiration (90% with scrubland, rainfed crops, irrigated rice representing the largest share), discharge at the outlet (5.6%), additional groundwater storage (1.6%), reservoir evaporation (2.5%), the remaining 0.3% corresponding to revaporation from the groundwater reservoir and additional storage in soils and reservoirs. Additional storage in groundwater, soil and tanks is due to the fact that the last year of simulation (2010) was a wet year; this is certainly not representative of a long-term trend.

The total recharge and the water extraction computed in SWAT are presented for each sub-basin in Fig. 8. The potential water extraction (Table 4) is the amount of irrigation defined as an input: it is the potential amount of irrigation per day for each day of irrigation for each irrigation plot. This irrigation amount is fixed over the simulation period and determined by the land use map. In contrast, the simulated water extraction depends on the groundwater

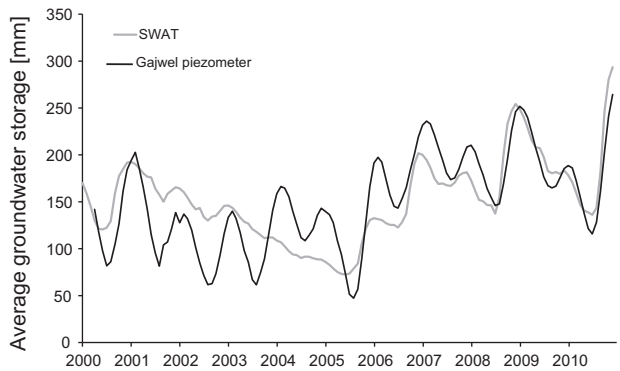

Fig. 6. Average monthly groundwater storage simulated with the calibrated model compared with groundwater storage computed from monthly piezometric data from AP Groundwater Department using local values of aquifer thickness and specific yield.

availability simulated in each sub-basin and the crops demand. Therefore, simulated water extraction may be less than potential extraction especially after dry years with limited recharge (Fig. 4c). This is the case in 2008 and 2010 as a consequence of the dry monsoons of 2007 and 2009.

The simulated natural recharge and return flow from excess irrigation (Table 4) is variable across sub-basins. The model produces 56% more natural recharge and return flow for the sub-basin 8 (134.6 mm/year) than for the sub-basin 10 (84.9 mm/year) on annual average over the period of simulation. The spatial variability is explained by (i) the difference in irrigated surfaces in each sub-basin because the return flow represents a significant contribution to the total recharge, (ii) the different repartitions of land use across sub-basins, some favoring natural recharge (e.g., rainfed crops) others limiting natural recharge (e.g., scrubland), (iii) tank seepage that is comprised between 31.9 and 67.9 mm/year depending on the tank density in each sub-basin and the runoff amount generated.

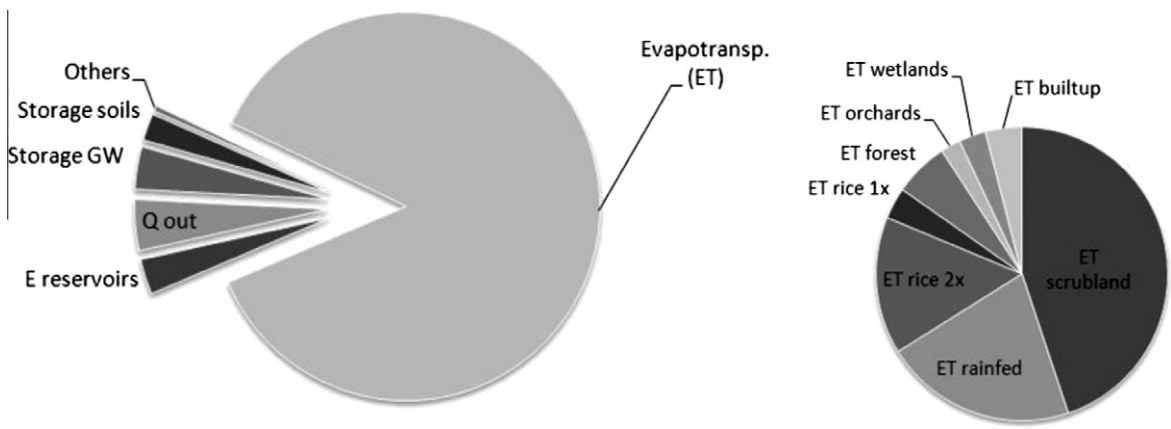

Fig. 7. Redistribution of the mean annual rainfall in the different sub-systems at watershed scale (simulation period 2000–2010). The right graph shows the repartition of evapotranspiration for the different land covers.

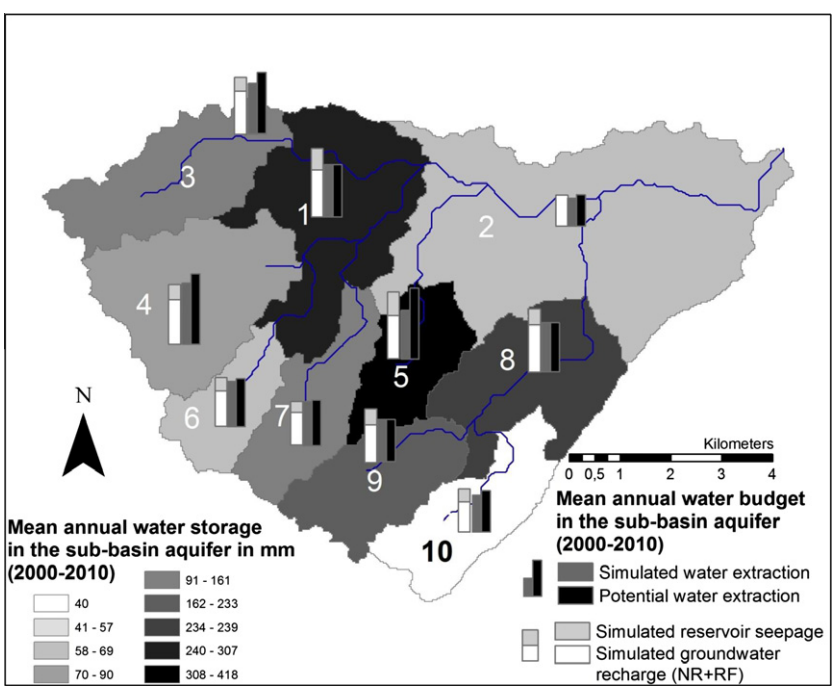

Fig. 8. Mapping of average annual groundwater storage, groundwater extraction and recharge per sub-basin, simulation period 2000–2010.

The simulated mean annual groundwater storage presents also a high variability between sub-basins (Table 4), from 40 mm (sub-basin 10) to 418 mm (sub-basin 5). The spatial variability of the mean annual groundwater storage (Fig. 8) is due to the combined effects of the storage capacity of each sub-basin (Fig. 2a) and the difference between the simulated water extraction and total aquifer recharge: sub-basins in the upstream part have generally low groundwater reserves because of a limited storage capacity and extraction matching recharge; in contrast sub-basins in the central part of the watershed have significantly higher reserves because of better storage capacity associated with a positive balance between recharge and extraction. This is indicative of a non-optimal geographical distribution of extractions in the watershed with upstream areas under higher water stress than downstream.

The estimated maximal storage capacity of the percolation tanks (5.4 Mm^3, Table 1) is about 10% of the aquifer storage capacity over the Gajwel basin (52.4 Mm^3, Table 4) and the tanks contribute on average for the period 2000–2010 to 43% (2.75 Mm^3) of the aquifer recharge (without irrigation return flows) and 25% of annual groundwater extraction. This recharge contribution is higher in dry years (54%, year 2007) compared to wet years (32%, year 2008) (Fig. 4). The relative contribution of tank seepage to the recharge is likely over-estimated in dry years because natural recharge is not properly simulated.

Percolation tank water losses occur by evaporation (1.6 Mm^3/year or 19.6 mm/year) and by overflow feeding the watershed outlet (1.6 Mm^3/year or 19.5 mm/year). Moreover, runoff occurring in the downstream sub-basin (no. 2, Fig. 2a) is not captured by tanks and this represents a volume of water of 2.06 Mm^3/year (24.5 mm/year) at the outlet.

5. Discussion

The SWAT modeling framework was applied to an agricultural watershed with both irrigated and rainfed crops, surface reservoirs capturing runoff and contributing to aquifer recharge, groundwater reservoirs as the main water resource, and no perennial streams. Unlike more classical applications where calibration is based on stream/river fluxes data, in the present study the calibration was based on surface reservoir storage for runoff and recharge derived from the groundwater balance for groundwater reservoirs.

Overall the modeling approach using SWAT reproduces recharge estimates derived from the groundwater balance (Fig. 4). Simulated runoff is also close to the observed one (Fig. 5) and reservoirs capture all the runoff during dry years (2001–2004, 2007, 2009) and allow only limited amounts of overflow during wet years (6 mm, 46 mm, 42 mm, 98 mm, 20 mm in 2000, 2005, 2006, 2008, 2010 respectively) similarly to visual observations in the field (tank levels and flow at the outlet) with the noticeable exception of the monsoon 2008 for which simulated runoff is likely over-estimated. The model captures reasonably well the groundwater dynamics as observed by using piezometric time series (Fig. 6).

The calibration step should not be overlooked for an appropriate application of SWAT for water resource availability assessment and a series of field data (aquifer geometry, piezometric data, reservoirs geometry and dynamics, independently-derived recharge estimates, runoff information, etc.) are needed. Usually the river discharge is the main available information used to calibrate runoff and base flow from groundwater. The share between recharge and evapotranspiration is thus deduced but not calibrated. In semi-arid or arid areas, river discharge is not the major hydrological transfer. For instance the study by Bouwer et al. (2008) focused on model calibration based on ET data derived from satellite imagery only. Immerzel and Droogers (2008) have shown that the calibration of SWAT HRU using such data is limited by the incertitude of evapotranspiration estimates from satellite imagery and also that actual evapotranspiration was more sensitive to the groundwater and meteorological parameters than the soil and land use parameters. They have constrained the climatic and soil/plant model parameters with their approach, but no data/calibration on the aquifer and tanks is available for this 8 months period study. However using evaporation patterns derived from satellite imagery could be a complementary method to obtain additional information for the estimation of the spatial water budget in our study site.

In SWAT, the aquifer system has to be conceptualized in the form of individual reservoirs for each sub-basin, which are hydraulically independent of each other. This is not a significant constraint in the local context because lateral groundwater fluxes are small compared to vertical fluxes (recharge, return flow, pumping) for two main reasons: groundwater pumping is evenly distributed at kilometric scale, and the low water table contributes to the compartmentalization of the aquifer system (i.e., the saprolite layer, which has continuity at kilometer scale is mostly unsaturated under present conditions).

Therefore lumped reservoir modeling is well adapted in complex crystalline aquifer systems and has been used recently to simulate groundwater balance and long-term trends in groundwater levels (Dewandel et al., 2010) and groundwater quality (Perrin et al., 2011a). Independent groundwater reservoirs need to be of reasonable size (>0.5–1 km^2) to ensure the dominance of vertical fluxes over lateral ones (Dewandel et al., 2012). It should however be emphasized that such modeling approach with independent groundwater reservoirs may not be applicable to other hydrogeological settings presenting for instance more permeable and/or thicker aquifers permitting substantial horizontal groundwater flow components.

However some limitations of the model have been observed: Runoff and recharge were underestimated during dry years leading to an overestimation of evapotranspiration. It was difficult to reproduce the natural recharge variability between dry and humid years. This may be due to the bimodal soil type occurring in the region (de Condappa et al., 2008) which may favor preferential flow in dry years and proportionally retain more infiltration in wet years. These processes, however, cannot be reproduced with the SWAT conceptual model of soils. Runoff is also not well simulated in some cases: for the monsoon 2007, runoff occurs too early in the simulation and the observed significant runoff occurring later is not reproduced (Fig. 5); in contrast simulated runoff for the monsoon 2008 seems to be higher than actual. The Curve Number empirical approach at a daily time step used for the modeling has not the capacity to reproduce different types of runoff events for which rainfall intensity and distribution is likely to be significant.

Other uncertainties are borne by field-derived data, especially the land use: it is observed that irrigated crop areas as well as rainfed crop areas may vary according to the water availability: farmers try to optimize the utilization of their water resource according to the intensity of the monsoon and the discharge of their wells (discharge decreases when groundwater levels are low, e.g. Perrin et al., 2011b). A static land use is used in the model and groundwater extraction is estimated from statistical data published by the Government and not by direct measurements/observations (Table 2); therefore this uncertainty is present both in the model and in the groundwater balance. In fact, to some extent the model may be closer to actual extractions because it adjusts the groundwater extraction to the available water resource resulting in a water extraction that is less than the potential water extraction (Table 4) and less than the groundwater extraction used for the groundwater balance. A temporal data set of land use imagery

Table 4
Sub-basin main characteristics and average simulated groundwater fluxes and storage for the simulation period 2000–2010.

Sub-basin ID	Area (km^2)	Model input data (field campaigns 2009–2010)						Model simulation results (average annual value 2000–2010)				
		Maximal groundwater capacity (mm)	Rice cultivated twice (%-subb. area)	Rice cultivated once (%-subb. area)	Orchards (%-subb. area)	Potential groundwater extraction (mm)	Initial water volume (mm)	Actual groundwater extraction (mm)	Natural recharge + return flow (mm)	Tank seepage (mm)	Groundwater storage (mm)	Minimum and maximum monthly groundwater volume (mm)
1	10.7	750	6.92	3.22	0.00	152	368	152	132.7	62.5	307	219–631
2	23.6	569	3.88	2.16	0.00	92	204	81	88.6	0.0	61	1.6–161
3	7.4	503	8.79	3.27	0.00	178	146	146	123.0	39.4	161	6.8–229
4	9.5	702	13.47	3.06	2.68	204	365	178	127.3	42.8	76	0–252
5	4.5	956	8.41	2.14	2.18	207	356	142	122.7	67.9	418	141–600
6	3.8	528	8.27	3.70	3.24	140	216	132	100.0	38.6	61	0–217
7	5.4	585	9.21	1.58	3.82	133	382	129	91.7	31.9	102	18–260
8	7.7	819	6.99	2.70	0.00	143	325	143	134.6	46.0	239	177–585
9	5.7	402	6.81	1.81	0.52	122	285	122	108.1	43.8	233	142–402
10	5.8	433	9.39	1.92	3.39	120	118	106	84.9	36.6	40	0–211

would have to be used to better take into account the pumping temporal variability.

In most studies, SWAT is applied to reproduce river flow with modeling efforts focusing on runoff and baseflow whereas recharge and evaporation fluxes are less constrained (e.g., Eckhardt and Ulbrich, 2003; Bouraoui et al., 2004; Gosain et al., 2005). In this study, recharge was a key parameter for calibration. It showed that the model was limited in reproducing adequately the recharge inter-annual variability with evaporation flux being over-estimated in dry years at the expense of recharge and runoff.

Reservoir evaporation and flow at the outlet may be considered as unused available water and account for 64 mm/year on average for the simulated period 2000–2010 (Fig. 7). It does not mean that this amount is readily available: it is necessary to preserve flow at the outlet for downstream users (Batchelor et al., 2003; Kumar et al., 2006), and more efficient use of water stored in tanks (Perrin et al., 2009) would reduce evaporation loss but not suppress it completely. Another important aspect is that this excess water is observed only during wet years when water-stress is virtually non-existent in the watershed. For the dry years 2007 and 2009, the losses at the outlet are 2.6 mm and 8 mm respectively, and the tank evaporation losses 15 mm and 11 mm. This argues for optimizing (i.e., maximizing) the use of surface water in wet years so as to preserve groundwater resource as a supplementary resource for dry years.

Water availability in the watershed is far from homogeneous as shown by the variability between sub-basins (Fig. 8): the aquifer geometry makes the initial water volume in each reservoir highly variable (118–382 mm, Table 4), because of contrasted land use the groundwater extraction mostly for rice irrigation is comprised between 92 and 207 mm/year (Table 4) and does not match the aquifer storage capacity (i.e., no correlation between aquifer storage and water extraction in each sub-basin). Moreover the total aquifer recharge is highly variable between sub-basins because of the land use and the repartition of percolation tanks (Table 4, Fig. 2c). This spatial variability has consequences on the agriculture production with as much as 40% rice yield reduction in the sub-basins under water-stress during drought years. Therefore the water availability mapping (Fig. 8) may be used to investigate farmer vulnerability for instance. The sub-basin limits are however conceptual and the actual spatial variability may be smoother than the modeled one as lateral connections between sub-basins may exist especially in areas with lower density of pumping wells.

In future studies, the model calibration could be improved by acquiring additional data sets: land use time series to better define crop rotations and farming practices (irrigation amounts), satellite imagery to derive a spatial distribution of evapotranspiration from scrub-lands, forested areas, rainfed crops, and information on the daily rainfall–runoff relationship.

6. Conclusions

The integrated surface water–groundwater resource modeling of a small hard-rock semi-arid watershed of southern India proved to be successful using SWAT. The model provides semi-distributed outputs at HRU and sub-basin scales, which help to visualize spatial variability in water fluxes and water availability. It also offers easy implementation and simulation of water use scenarios according to land use or climate change scenarios (e.g., Kumar et al., 2006). One limitation of the model was the simulation of recharge and runoff during wet years that remained higher than observed.

Results show that evapotranspiration is by far the largest water flux and the role of percolation tanks is significant as it provides about 23% of the annual aquifer recharge (or 33% of the recharge without including irrigation return flows) for normal monsoons. However the tank contribution to recharge is highly variable spatially as a consequence of uneven tank repartition. Scope for additional managed aquifer recharge is limited as a significant share of the runoff is already captured and there is a need to provide "blue" water to the downstream users. The water balance is highly variable inter-annually because of the contrasted monsoon intensity. In dry years, water-stress occurs in the entire watershed but in a contrasted manner across watersheds depending on the respective groundwater reservoir capacity, land use, percolation tanks distribution. This has an impact on the agricultural production with a significant decrease in crop yields during dry years. Therefore water resource management measures are needed in order to limit negative climatic impacts on the farming economy: maximizing surface water usage (direct use from surface tanks, rainfed crops) and preservation of groundwater reserves to be used as a supplementary resource in dry years may provide an optimized approach. This would however require demand-management measures (less pumping) and community-based water resource management.

It is planned to use the same modeling approach at a more regional scale (1000 km^2) and investigate the impact of scenarios integrating global changes (climate, land use) on the water resource and to assess the vulnerability of rural water users to these changes.

Acknowledgments

We would like to thank ICRISAT for sharing their meteorological data. We are grateful to the French Ministry of Foreign Affairs and the Embassy in India Cooperation and Cultural Service for their support and the funding of missions of French scientists. This work has been supported by the French Research National Agency (ANR) through its VMCS program (Project SHIVA No. ANR-08-VULN-10-01). We are grateful to the Associate Editor and three anonymous reviewers for their insightful remarks and comments that improved the manuscript.

References

Ahmad, M., Bastiaanssen, W.G.M., Feddes, R.A., 2005. A new technique to estimate net groundwater use across large irrigated areas by combining remote sensing and water balance approaches, Rechna Doab, Pakistan. Hydrogeol. J. 13, 653–664. http://dx.doi.org/10.1007/s10040-004-0394-5.

Anuraga, T.S., Ruiz, L., Mohan Kumar, M.S., Sekhar, M., Leijnse, A., 2006. Estimating groundwater recharge using land use and soil data: a case study in South India. Agric. Water Manag. 84, 65–76. http://dx.doi.org/10.1016/j.agwat.2006.01.017.

Arnold, J.G., Allen, P.M., 1996. Estimating hydrologic budgets for three Illinois watersheds. J. Hydrol. 176, 57–77.

Batchelor, C.H., Rama Mohan Rao, M.S., Manohar Rao, S., 2003. Watershed development: a solution to water shortages in semi-arid India or part of the problem? Land Use Water Resour. Res. 3, 1–10.

Borah, D.K., Bera, M., 2004. Watershed-scale hydrologic and nonpoint-source pollution models: review of applications. Am. Soc. Agric. Eng. 47, 789–803 (ISSN 0001-2351).

Bouraoui, F., Grizzetti, B., Granlund, K., Rekolainen, S., Bidoglio, G., 2004. Impact of climate change on the water cycle and nutrient losses in a Finnish catchment. Climatic Change 66 (1), 109–126.

Bouwer, L.M., Biggs, T.W., Aerts, J.C.J.H., 2008. Estimates of spatial variation in evaporation using satellite-derived surface temperature and a water balance model. Hydrol. Process. 22, 670–682.

Central Ground Water Board, 2005. Master Plan for Artificial Recharge to Ground Water in India. New Delhi: Government of India, Ministry of Water Resources. <http://cgwb.gov.in/documents/MASTER PLAN Final-2002.pdf>.

Central Ground Water Board, 2007. Manual on Artificial Recharge of Ground Water, 185 p. <http://cgwb.gov.in/documents/Manual on Artificial Recharge of Ground Water.pdf>.

Chaplot, V., 2007. Water and soil resources response to rising levels of atmospheric CO_2 concentration and to changes in precipitation and air temperature. J. Hydrol. 337, 159–171.

Chowdary, V.M., Rao, N.H., Sarma, P.B.S., 2003. GIS-based decision support system for groundwater assessment in large irrigation project areas. Agric. Water Manag. 62, 229–252. http://dx.doi.org/10.1016/S0378-3774(03)00144-6.

Coudrain-Ribstein, A., Pratx, B., Talbi, A., Jusserand, C., 1998. Is the evaporation from phreatic aquifers in arid zones independent of the soil characteristics? C. R. Acad. Sci. Paris, Sci. Terre Planèt. 326, 159–165.

De Condappa, D., 2005. Study of the Spatialized Water Flow Processes of the Vadose Zone of Hard-rock Aquifers. Implementation for the Evaluation of the Recharge at the Watershed Scale, Maheshwaram Watershed, Andhra Pradesh, India (in French). PhD Thesis, University of Grenoble, France, 355 p.

De Condappa, D., Galle, S., Dewandel, B., Haverkamp, R., 2008. Bimodal zone of the soil textural triangle: common in tropical and subtropical regions. Soil Sci. Soc. Am. J. 72, 33–40. http://dx.doi.org/10.2136/sssaj2006.0343.

Dewandel, B., Lachassagne, P., Wyns, R., Maréchal, J.C., Krishnamurthy, N.S., 2006. A generalized 3-D geological and hydrogeological conceptual model of granite aquifers controlled by a single or multiple weathering. J. Hydrol. 330, 260–284.

Dewandel, B., Gandolfi, J.-M., Ahmed, S., Subrahmanyam, K., 2007. A decision support tool for sustainable groundwater management in semi-arid hard-rock areas with variable agro-climatic scenarios. Curr. Sci. India 92, 1093–1102.

Dewandel, B., Gandolfi, J.M., de Condappa, D., Ahmed, S., 2008. An efficient methodology for estimating irrigation return flow coefficients of irrigated crops at watershed and seasonal scales. Hydrol. Process. 22 (11), 1700–1712.

Dewandel, B., Perrin, J., Ahmed, S., Aulong, S., Hrkal, Z., Lachassagne, P., Samad, M., Massuel, S., 2010. Development of a Tool for managing groundwater resources in semi-arid hard-rock regions. Application to a rural watershed in south India. Hydrol. Process. 24, 2784–2797. http://dx.doi.org/10.1002/hyp.7696.

Dewandel, B., Maréchal, J.C., Bour, O., Ladouche, B., Ahmed, S., Chandra, S., Pauwels, H., 2012. Upscaling and regionalizing hydraulic conductivity and effective porosity at watershed scale in deeply weathered crystalline aquifers. J. Hydrol. 416–417, 83–97.

Dripps, W.R., Bradbury, K.R., 2010. The spatial and temporal variability of groundwater recharge in a forested basin in northern Wisconsin. Hydrol. Process. 24, 383–392. http://dx.doi.org/10.1002/hyp.7497.

Eckhardt, K., Ulbrich, U., 2003. Potential impacts of climate change on groundwater recharge and streamflow in a central European low mountain range. J. Hydrol. 284 (1–4), 244–252.

Faramarzi, M., Yang, H., Schulin, R., Abbaspour, K.C., 2010. Modeling wheat yield and crop water productivity in Iran: implications of agricultural water management for wheat production. Agric. Water Manag. 97, 1861–1875.

Glendenning, C.J., Vervoort, R.W., 2011. Hydrological impacts of rainwater harvesting (RWH) in a case study catchment: the Arvari River, Rajasthan, India. Part 2. Catchment-scale impacts. Agric. Water Manag. 98, 715–730.

Gosain, A.K., Rao, S., Srinivasan, R., Gopal Reddy, N., 2005. Return-flow assessment for irrigation command in the Palleru river basin using SWAT model. Hydrol. Process. 19, 673–682. http://dx.doi.org/10.1002/hyp.5622.

Immerzel, W.W., Droogers, P., 2008. Calibration of a distributed hydrological model based on satellite evapotranspiration. J. Hydrol. 349, 411–424. http://dx.doi.org/10.1016/j.jhydrol.2007.11.017.

Kay, M., Franks, T., Smith, L.E.D., 1997. Water: Economics, Management and Demand. Chapman Hall, London.

Kumar, M.D., 2003. Food Security and Sustainable Agriculture in India: The Water Management Challenge. Colombo, Sri Lanka: International Water Management Institute (Working Paper 60).

Kumar, M.D., 2005. Impact of electricity prices and volumetric water allocation on energy and groundwater demand management: analysis from Western India. Energy Policy 33, 39–51. http://dx.doi.org/10.1016/S0301-4215(03)00196-4.

Kumar, K.R., Sahai, A.K., Krishna Kumar, K., Patwardhan, S.K., Mishra, P.K., Revadekar, J.V., Kamala, K., Pant, G.B., 2006. High-resolution climate change scenarios for India for the 21st century. Curr. Sci. 90 (3), 334–345.

Maréchal, J.C., Dewandel, B., Ahmed, S., Galeazzi, L., Zaidi, F.K., 2006. Combined estimation of specific yield and natural recharge in semi-arid groundwater basin with irrigated agriculture. J. Hydrol. 329, 281–293. http://dx.doi.org/10.1016/j.jhydrol.2006.02.022.

Massuel, S., Perrin, J., Wajid, M., Mascre, C., Dewandel, B., 2008. A simple low-cost method to monitor duration of ground water pumping. Ground Water 47 (1), 141–145. http://dx.doi.org/10.1111/j.1745-6584.2008.00511.x.

Massuel, S., Perrin, J., Mascré, C., Wajiduddin, M., Ahmed, S., in preparation. Assessing percolation of a small reservoir in South India using a daily water balance approach. J. Hydrol.

Mukherji, A., 2007. The energy-irrigation nexus and its impact on groundwater markets in eastern Indo-Gangetic basin: evidence from West Bengal, India. Energy Policy 35, 6413–6430. http://dx.doi.org/10.1016/j.enpol.2007.08.019.

NBSS, 2000. Andhra Pradesh soil map, Scale 1:500,000 – 6 Sheets. National Bureau of Soil Survey and Land Use Planning, ICAR, Nagpur, Publication 69.

Neitsch, S.L., Arnold, J.G., Kinry, J.R., Williams, J.R., 2002. Soil and Water Assessment Tool. Version 2000. Theoretical Documentation. USDA-ARS, Temple, Texas.

O'Brien, K., Leichenko, R., Kelkar, U., Venema, H., Aandahl, G., Tompkins, H., Javed, A., Bhadwal, S., Barg, S., Nygaard, L., West, J., 2004. Mapping vulnerability to multiple stressors: climate change and globalization in India. Global Environ. Change 14, 303–313. http://dx.doi.org/10.1016/j.gloenvcha.2004.01.001.

Perrin, J., Dewandel, B., Aulong, S., Ahmed, S., Hrkal, Z., Krazny, J., Mascre, C., Massuel, S., Mukherji, A., Samad, M., 2008. SUSTWATER Project Final Scientific Report. BRGM Report RP-56913-FR, 137 p.+ Appendices, 92 ill., 20 tabl.

Perrin, J., Mascre, C., Massuel, S., Ahmed, S., 2009. Tank Management in Andhra Pradesh, India: Percolation vs. Irrigation. IAHS Publication 330, Joint International Conference, Hyderabad, September 2009, pp. 28–33.

Perrin, J., Mascré, C., Pauwels, H., Ahmed, S., 2011a. Solute recycling: an emerging threat to groundwater quality in southern India? J. Hydrol. 398, 144–154. http://dx.doi.org/10.1016/j.jhydrol.2010.12.024.

Perrin, J., Ahmed, S., Hunkeler, D., 2011b. The role of geological heterogeneities and piezometric fluctuations on groundwater flow and chemistry in hard-rock, southern India. Hydrogeol. J. 19 (6), 1189–1201. http://dx.doi.org/10.1007/s10040-011-0745-y.

Rangarajan, R., Athavale, R.N., 2000. Annual replenishable ground water potential of India—an estimate based on injected tritium studies. J. Hydrol. 234, 38–53.

Rosenberg, N.J., Brown, R.A., Izaurralde, R.C., Thomson, A.M., 2003. Integrated assessment of Hadley Centre (HadCM2) climate change projections on agricultural productivity and irrigation water supply in the conterminous United States: I. Climate change scenarios and impacts on irrigation water supply simulated with the HUMUS model. Agric. For. Meteorol. 117 (1–2), 73–96.

Ruud, N., Harter, T., Naugle, A., 2004. Estimation of groundwater pumping as closure to the water balance of a semi-arid, irrigated agricultural basin. J. Hydrol. 297, 51–73.

Sakthivadivel, R., 2007. The groundwater recharge movement in India. In: Giordano, Mark, Villholth, Karen G. (Eds.), The Agricultural Groundwater Revolution: Opportunities and Threats to Development. Comprehensive Assessment of Water Management in Agriculture Series. CABI Publishing, Wallingford, United Kingdom.

Shah, T., Bhatt, S., Shah, R.K., Talati, J., 2008. Groundwater governance through electricity supply management: assessing an innovative intervention in Gujarat, western India. Agric. Water Manag. 95, 1233–1242. http://dx.doi.org/10.1016/j.agwat.2008.04.006.

Sukhija, B.S., Reddy, D.V., Nagabhushanam, P.V., Hussain, S., 2003. Recharge processes: piston flow vs. preferential flow in semi-arid aquifers of India. Hydrogeol. J. 11, 387–395.

USDA-SCS, 1972. National Engineering Handbook, USDA-Soil Conservation Service.

USDA-SCS, 1983. National Engineering Handbook, Section 4 Hydrology (Chapter 19).

Williams, J.R., Jones, C.A., Dyke, P.T., 1984. A modeling approach to determining the relationship between erosion and soil productivity. Am. Soc. Agric. Eng. 27, 129–144.

World Bank, 2010. Deep wells and Prudence: Towards Pragmatic Actions for Addressing Groundwater Overexploitation in India, 97 p. <http://siteresources.worldbank.org/INDIAEXTN/Resources/2955831268190137195/DeepWellsGroundWaterMarch2010.pdf>.

Zaidi, F.K., Ahmed, S., Maréchal, J.C., Dewandel, B., 2007. Optimizing a piezometric network in the estimation of the groundwater budget: a case study from a crystalline-rock watershed in southern India. Hydrogeol. J. 15, 1131–1145.

Further reading

Shah, T., 2009. Taming the Anarchy: Groundwater Governance in South Asia, Resources for the Future. International Water Management Institute, Colombo, Washington, DC, 310p.